

Figure 4.1 Recording of action potential of an invertebrate nerve axon (a) An electronic stimulator supplies a brief pulse of current to the axon, strong enough to excite the axon. A recording of this activity is made at a downstream site via a penetrating micropipet. (b) The movement artifact is recorded as the tip of the micropipet drives through the membrane to record resting potential. A short time later, an electrical stimulus is delivered to the axon; its field effect is recorded instantaneously at downstream measurement site as the stimulus artifact. The action potential proceeds along the axon at a constant propagation velocity. The time period L is the *latent period* or transmission time from stimulus to recording site.

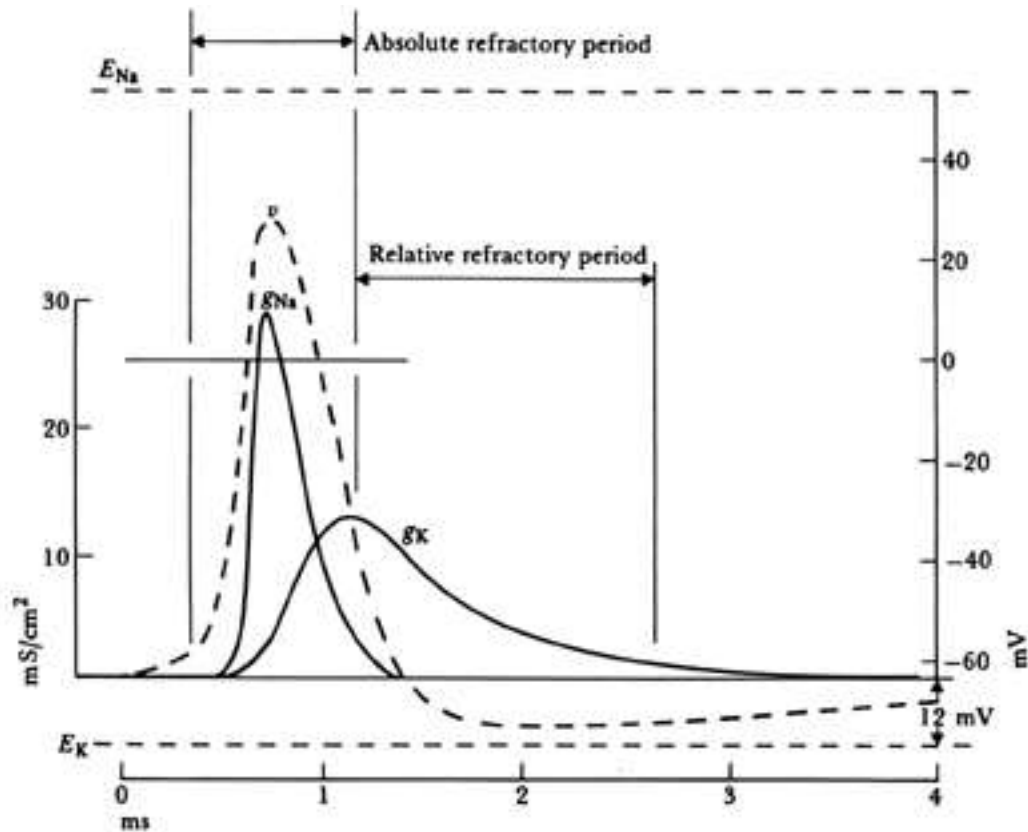


Figure 4.2 Theoretical action potential v and membrane ionic conductance changes for sodium (g_{Na}) and potassium (g_K) are obtained by solving the differential equations developed by Hodgkin and Huxley for the giant axon of the squid at a bathing medium temperature of 18.5 °C. E_{Na} and E_K are the Nernst equilibrium potentials for sodium and potassium across the membrane. (Modified from A. L. Hodgkin and A.F. Huxley, "A Quantitative Description of Membrane Current and Its Application to Conduction and Excitation in Nerve," *Journal of Physiology*, 1952, 117, p. 530.)

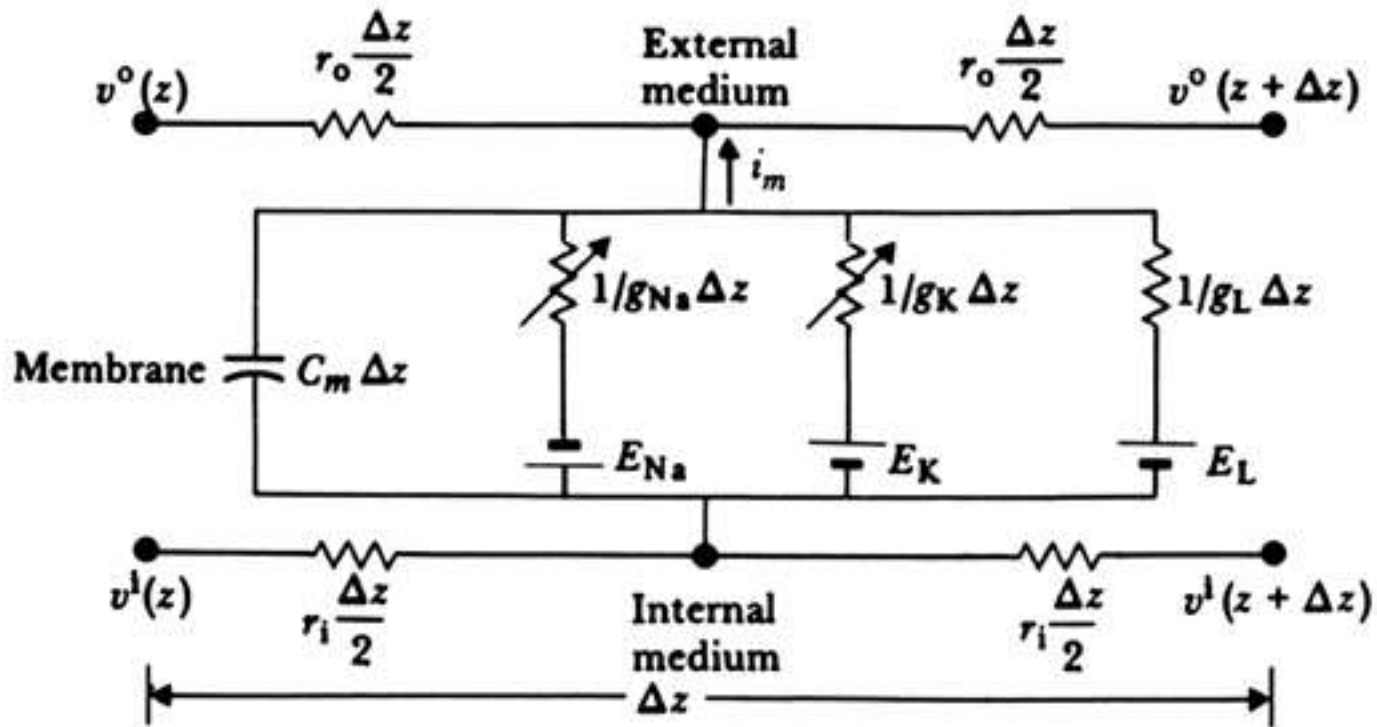


Figure 4.3 Diagram of network equivalent circuit of a small length (Δz) of an unmyelinated nerve fiber or a skeletal muscle fiber. The membrane proper is characterized by specific membrane capacitance C_m ($\mu\text{F}/\text{cm}^2$) and specific membrane conductances g_{Na} , g_{K} , and g_{Cl} in mS/cm^2 (millisiemens/ cm^2). Here an average specific leakage conductance is included that corresponds to ionic current from sources other than Na^+ and K^+ (for example, Cl^-). This term is usually neglected. The cell cytoplasm is considered simply resistive, as is the external bathing medium; these media may thus be characterized by the resistance per unit length r_i and r_o (Ω/cm), respectively. Here i_m is the transmembrane current per unit length (A/cm), and v^i and v^o are the internal and external potentials v at point z , respectively. (Modified from A. L. Hodgkin and A. F. Huxley, "A Quantitative Description of Membrane Current and Its Application to Conduction and Excitation in Nerve," *Journal of Physiology*, 1952, 117, p. 501.)

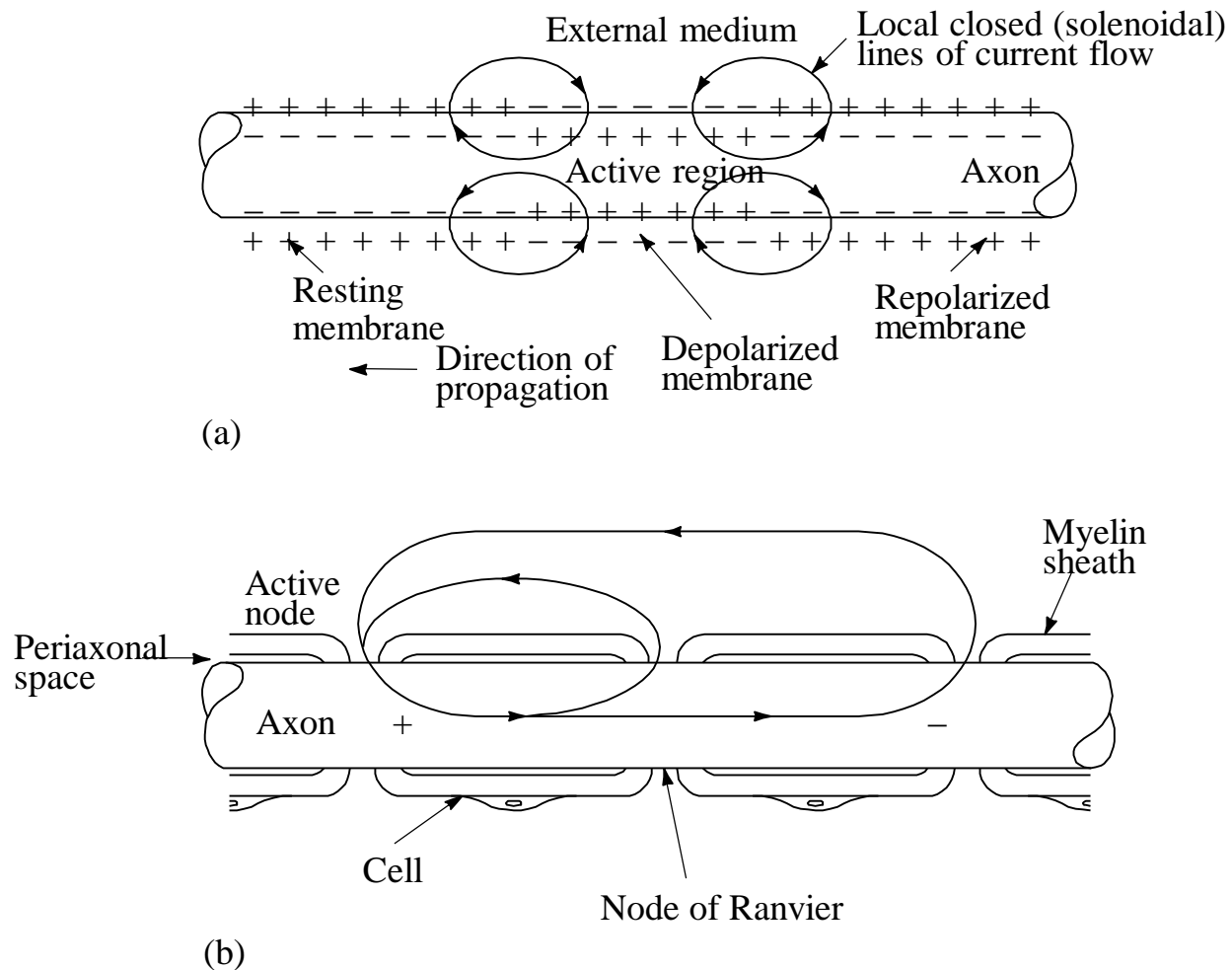
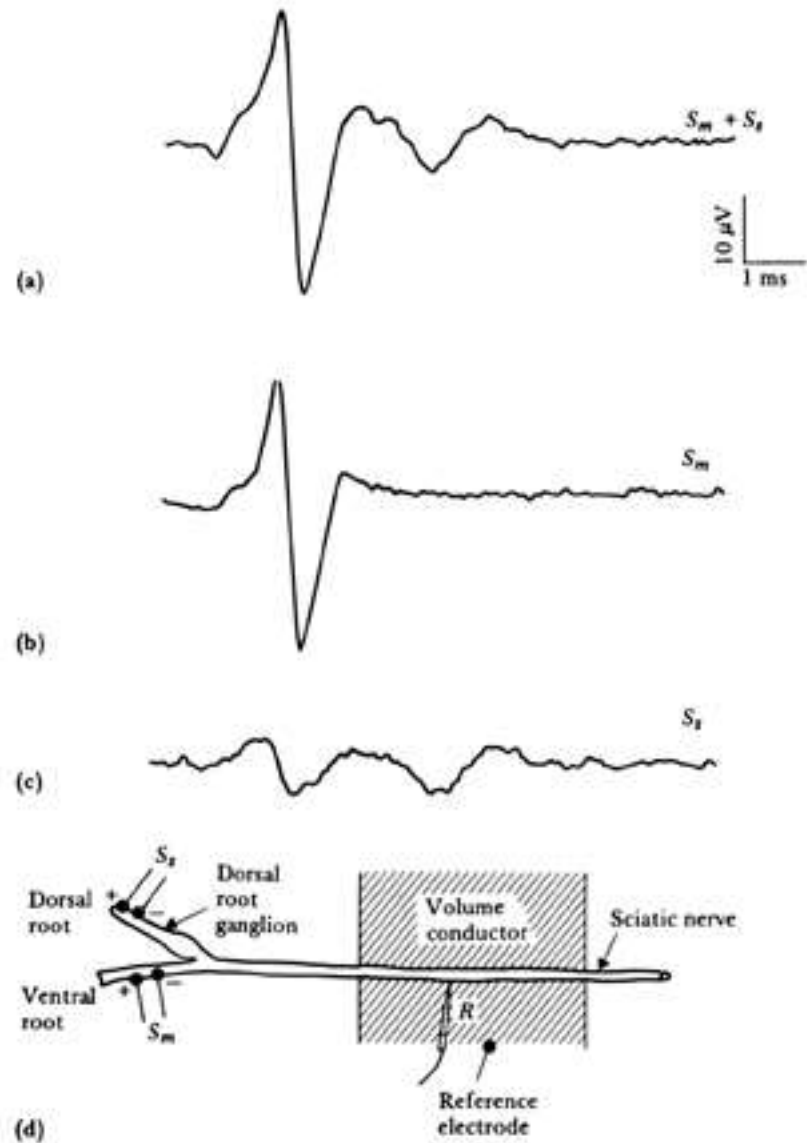


Figure 4.4 (a) Charge distribution in the vicinity of the active region of an unmyelinated fiber conducting an impulse. (b) Local circuit current flow in the myelinated nerve fiber.

Figure 4.5 Extracellular field potentials (average of 128 responses) were recorded at the surface of an active (1-mm-diameter) frog sciatic nerve in an extensive volume conductor. The potential was recorded with (a) both motor and sensory components excited ($S_m + S_s$), (b) only motor nerve components excited (S_m), and (c) only sensory nerve components excited (S_s).



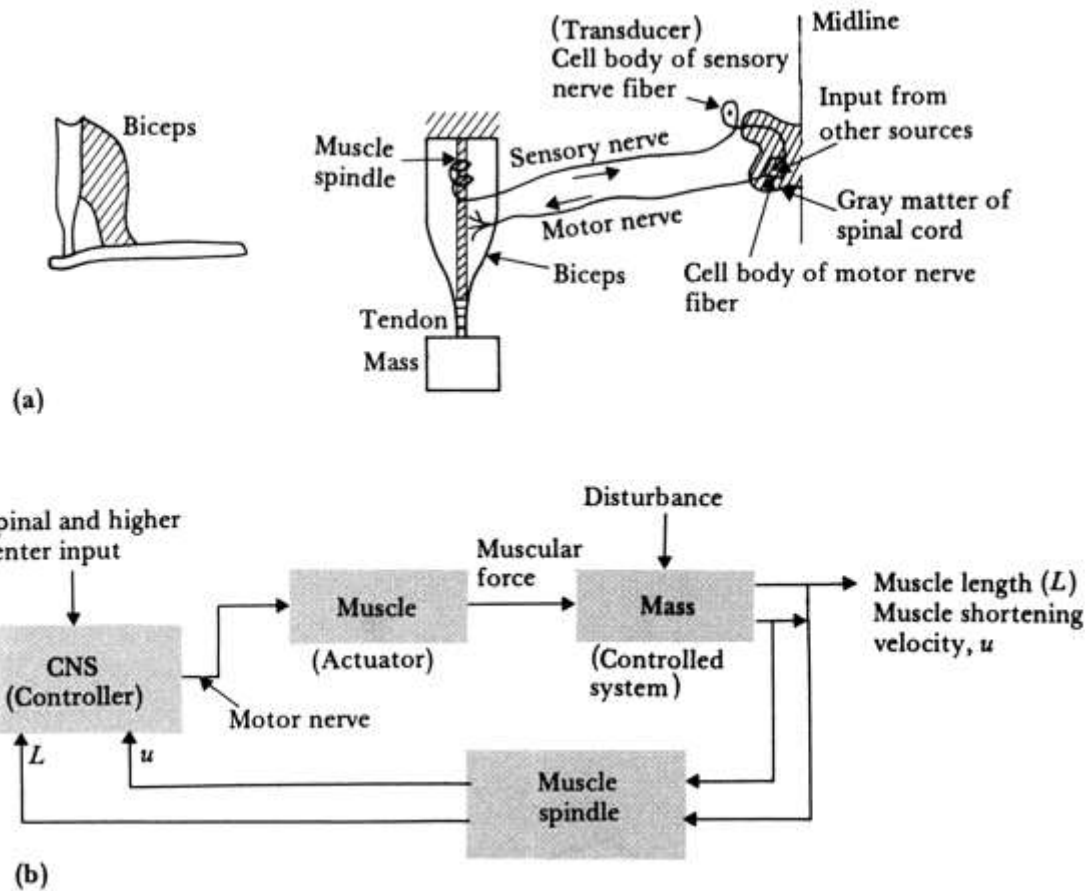


Figure 4.6 Schematic diagram of a muscle-length control system for a peripheral muscle (biceps) (a) Anatomical diagram of limb system, showing interconnections. (b) Block diagram of control system.

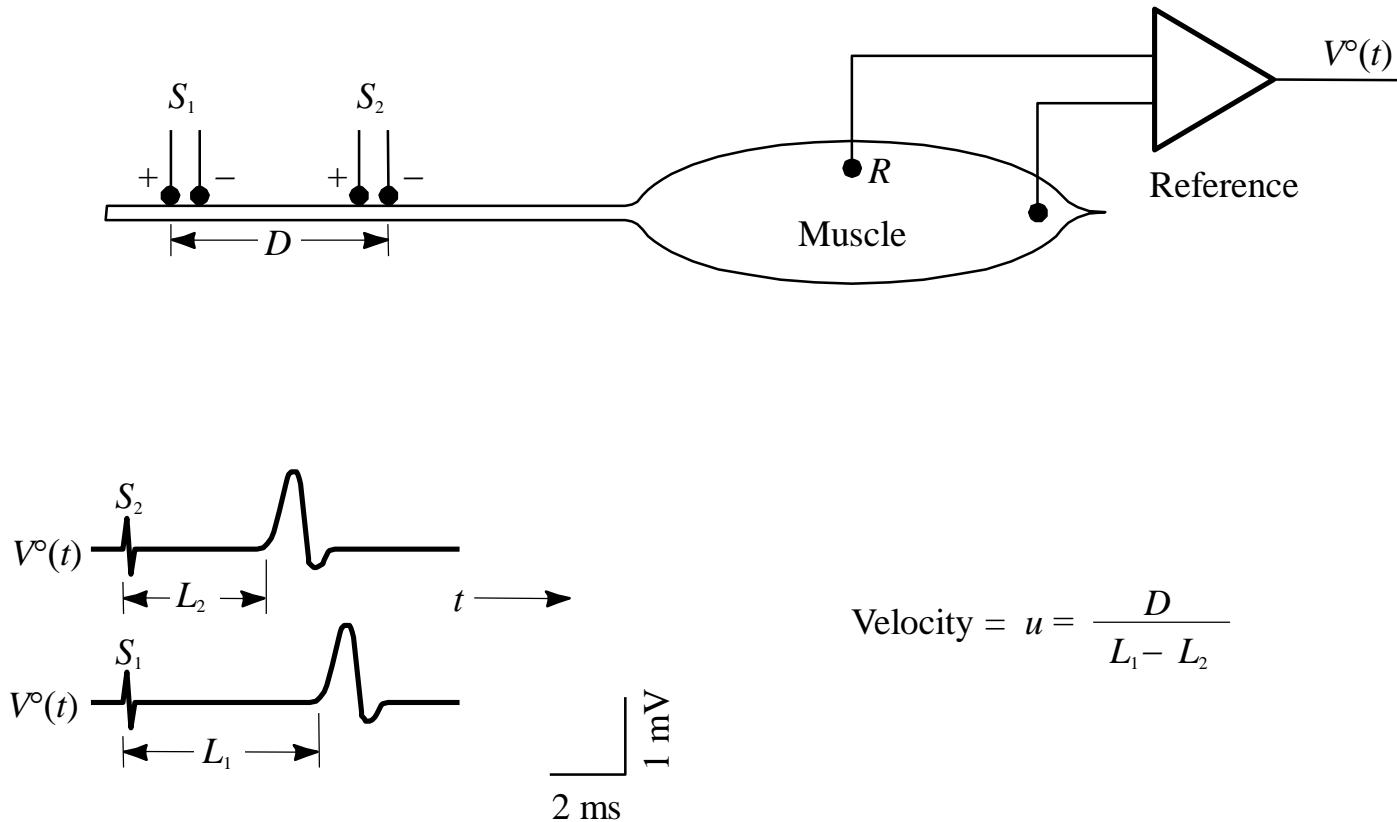


Figure 4.7 Measurement of neural conduction velocity via measurement of latency of evoked electrical response in muscle. The nerve was stimulated at two different sites a known distance D apart.

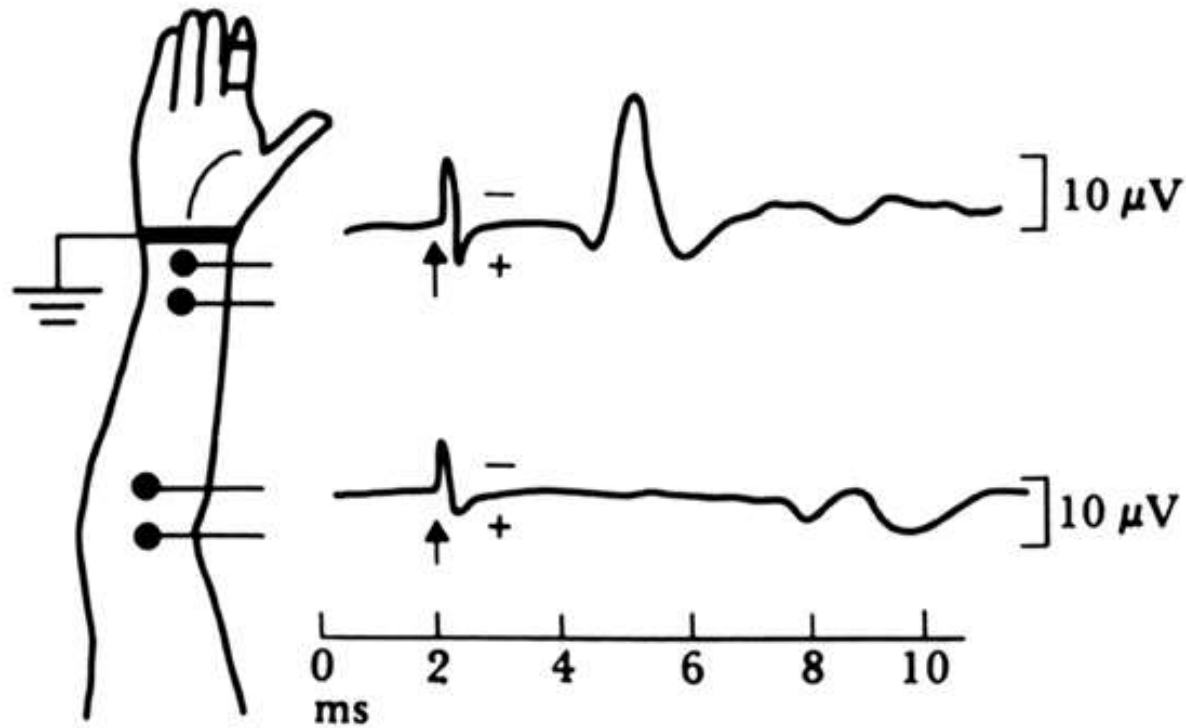


Figure 4.8 Sensory nerve action potentials evoked from median nerve of a healthy subject at elbow and wrist after stimulation of index finger with ring electrodes. The potential at the wrist is triphasic and of much larger magnitude than the delayed potential recorded at the elbow. Considering the median nerve to be of the same size and shape at the elbow as at the wrist, we find that the difference in magnitude and waveshape of the potentials is due to the size of the volume conductor at each location and the radial distance of the measurement point from the neural source. (From J. A. R. Lenman and A. E. Ritchie, *Clinical Electromyography*, 2nd ed., Philadelphia: Lippencott, 1977; reproduced by permission of the authors.)

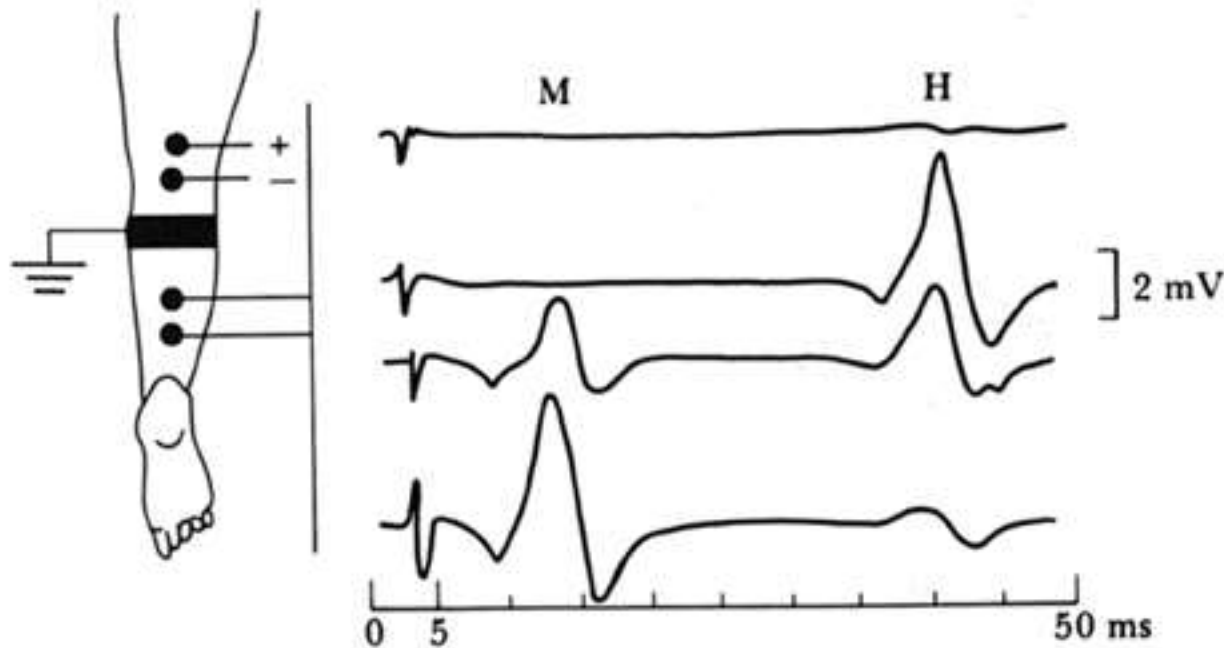


Figure 4.9 The H reflex The four traces show potentials evoked by stimulation of the medial popliteal nerve with pulses of increasing magnitude (the stimulus artifact increases with stimulus magnitude). The later potential or H wave is a low-threshold response, maximally evoked by a stimulus too weak to evoke the muscular response (M wave). As the M wave increases in magnitude, the H wave diminishes. (From J. A. R. Lenman and A. E. Ritchie, *Clinical Electromyography*, 2nd ed., Philadelphia: Lippincott, 1977; reproduced by permission of the authors.)

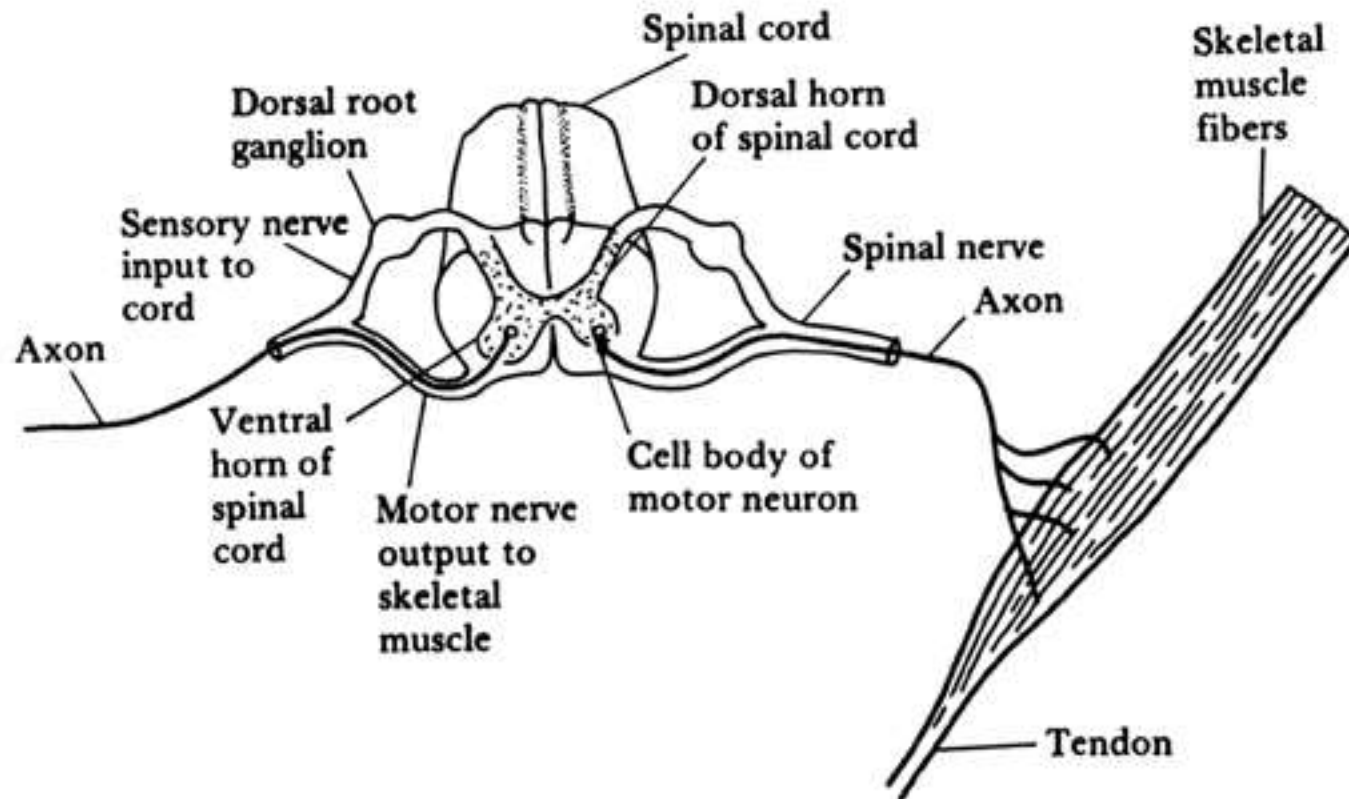
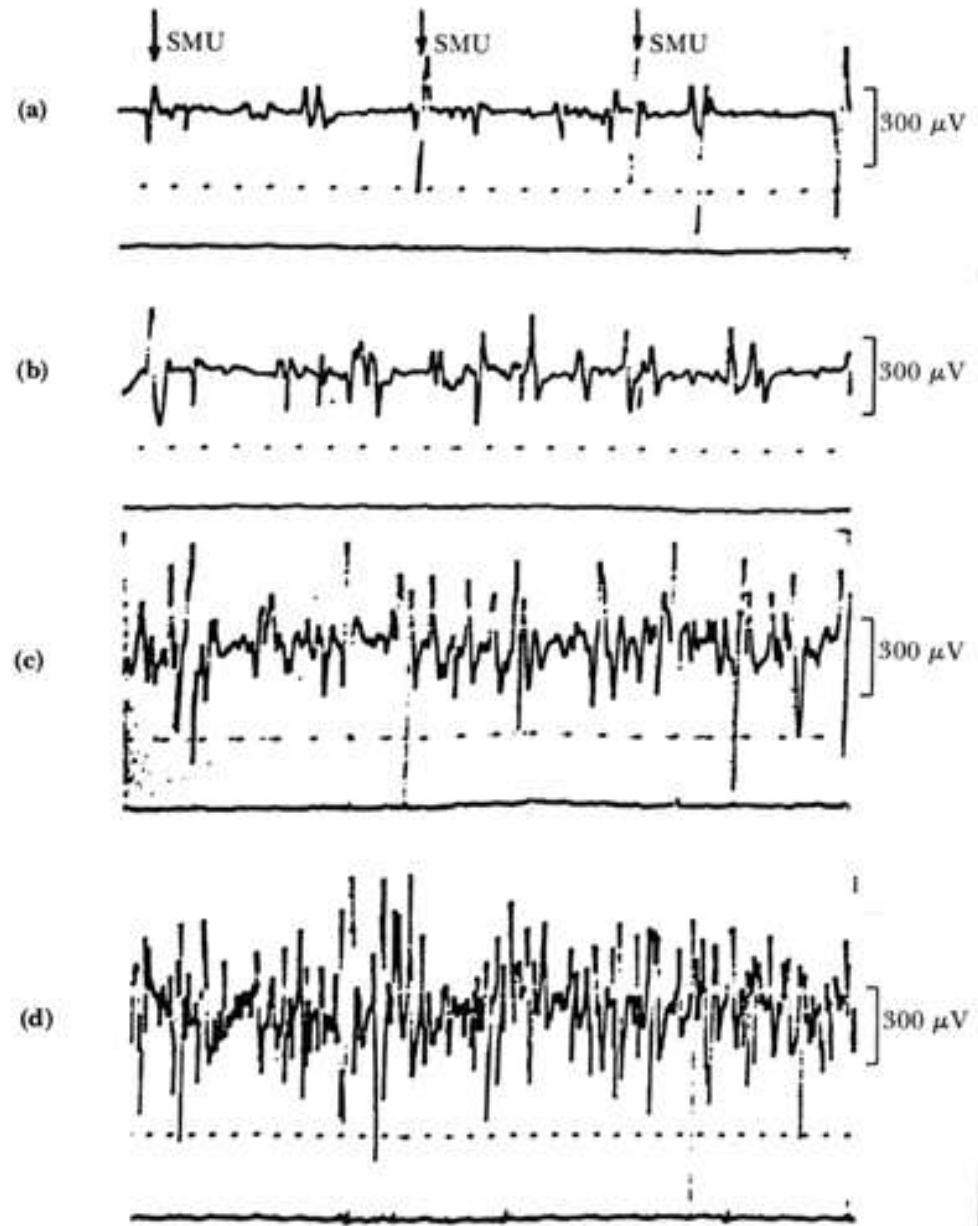


Figure 4.10 Diagram of a single motor unit (SMU), which consists of a single motoneuron and the group of skeletal muscle fibers that it innervates. Length transducers [muscle spindles, Figure 4.6(a)] in the muscle activate sensory nerve fibers whose cell bodies are located in the dorsal root ganglion. These bipolar neurons send axonal projections to the spinal cord that divide into a descending and an ascending branch. The descending branch enters into a simple reflex arc with the motor neuron, while the ascending branch conveys information regarding current muscle length to higher centers in the CNS via ascending nerve fiber tracts in the spinal cord and brain stem. These ascending pathways are discussed in Section 4.8.

Figure 4.11 Motor unit action potentials from normal dorsal interosseus muscle during progressively more powerful contractions. In the interference pattern (c), individual units can no longer be clearly distinguished. (d) Interference pattern during very strong muscular contraction. Time scale is 10 ms per dot. (From J. A. R. Lenman and A.E. Ritchie, *Clinical electromyography*, 2nd ed., Philadelphia: Lippincott, 1977; reproduced by permission of the authors.)



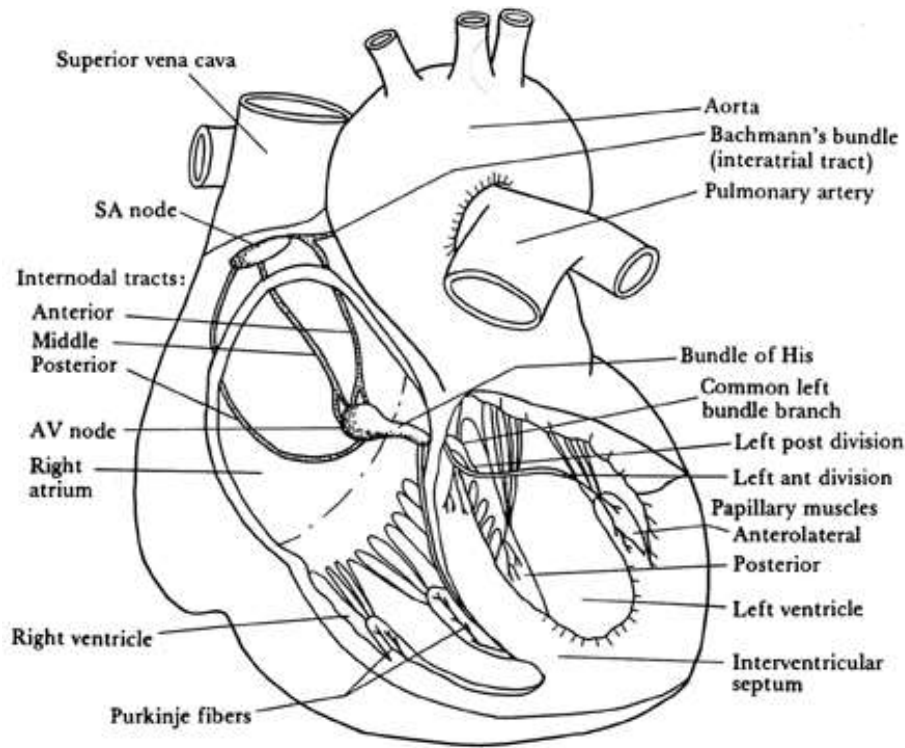


Figure 4.12 Distribution of specialized conductive tissues in the atria and ventricles, showing the impulse-forming and conduction system of the heart. The rhythmic cardiac impulse originates in pacemaking cells in the sinoatrial (SA) node, located at the junction of the superior vena cava and the right atrium. Note the three specialized pathways (anterior, middle, and posterior internodal tracts) between the SA and atrioventricular (AV) nodes. Bachmann's bundle (interatrial tract) comes off the anterior internodal tract leading to the left atrium. The impulse passes from the SA node in an organized manner through specialized conducting tracts in the atria to activate first the right and then the left atrium. Passage of the impulse is delayed at the AV node before it continues into the bundle of His, the right bundle branch, the common left bundle branch, the anterior and posterior divisions of the left bundle branch, and the Purkinje network. The right bundle branch runs along the right side of the interventricular septum to the apex of the right ventricle before it gives off significant branches. The left common bundle crosses to the left side of the septum and splits into the anterior division (which is thin and long and goes under the aortic valve in the outflow tract to the anterolateral papillary muscle) and the posterior division (which is wide and short and goes to the posterior papillary muscle lying in the inflow tract). (From B. S. Lipman, E. Massie, and R. E. Kleiger, *Clinical scalar Electrocardiography*. Copyright © 1972 by Yearbook Medical Publishers, Inc., Chicago. Used with permission. © From J. G. Webster (ed.), *Medical instrumentation: application and design*. 3rd ed. New York: John Wiley & Sons, 1998.

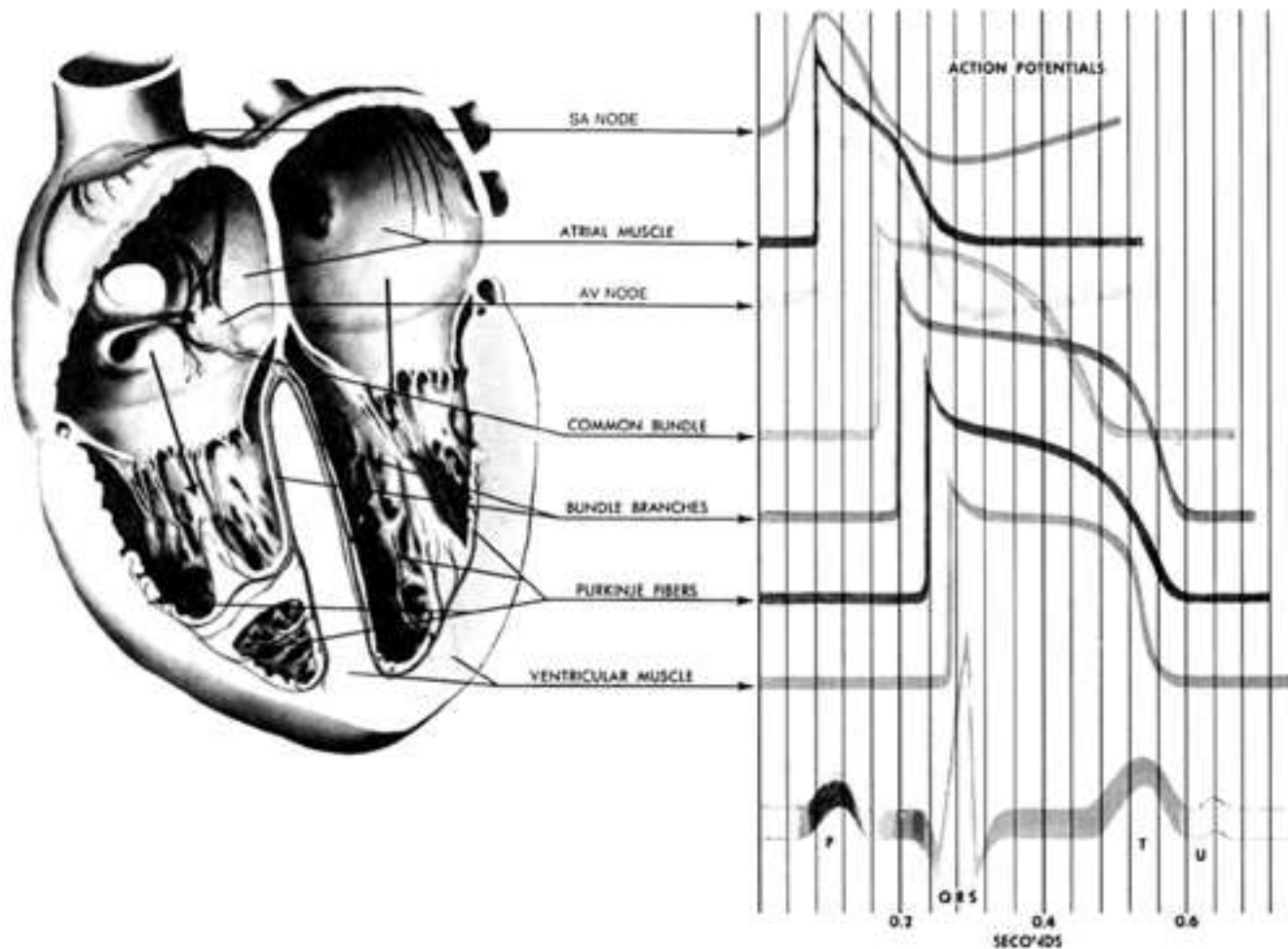


Figure 4.13 Representative electric activity from various regions of the heart. The bottom trace is a scalar ECG, which has a typical QRS amplitude of 1-3 mV. (© Copyright 1969 CIBA Pharmaceutical Company, Division of CIBAGEIGY Corp. Reproduced, with permission, from The Ciba Collection of *Medical Illustrations*, by Frank H. Netter, M. D. All rights reserved.)

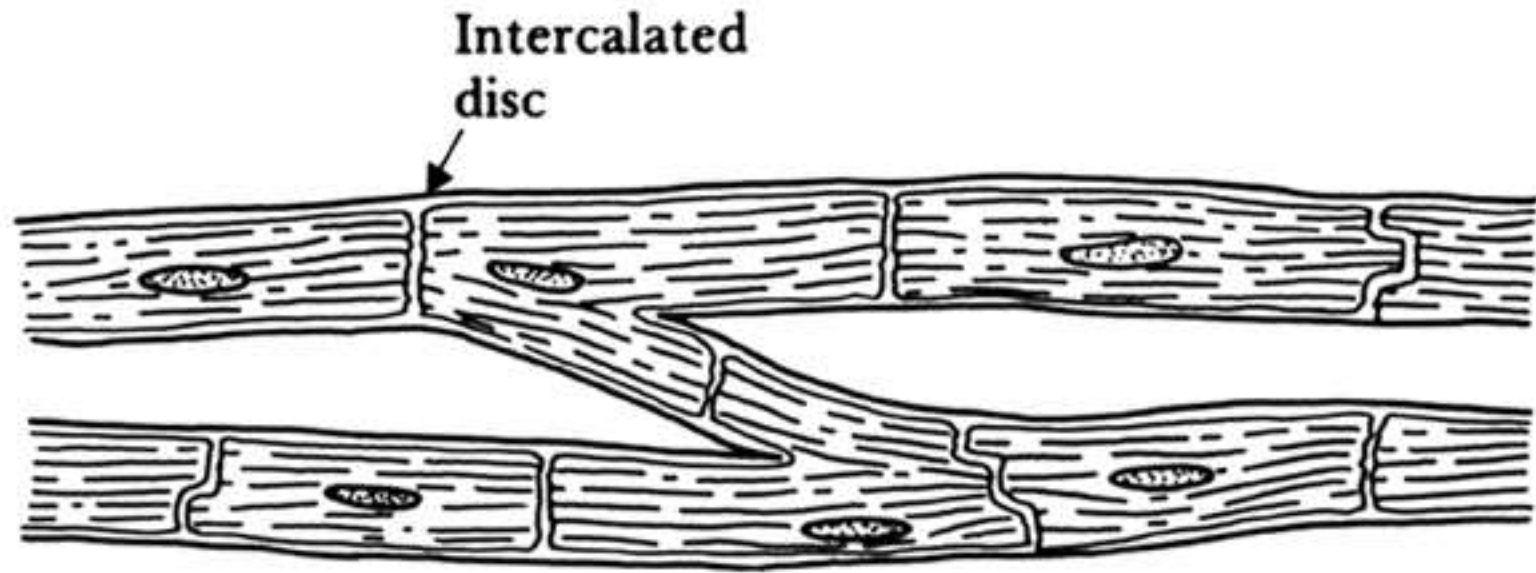


Figure 4.14 The cellular architecture of myocardial fibers Note the centroid nuclei and transverse intercalated disks between cells.

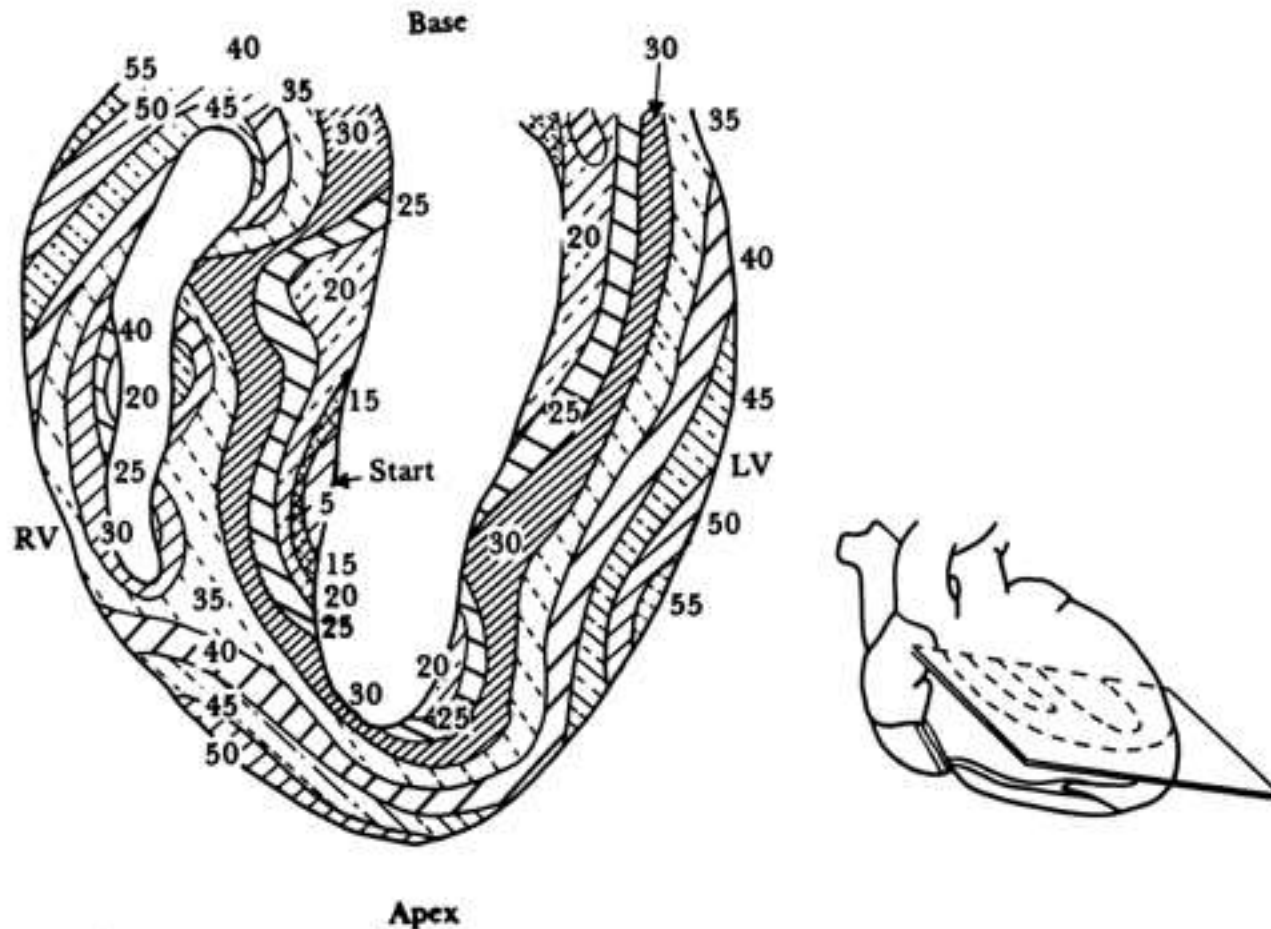


Figure 4.15 Isochronous lines of ventricular activation of the human heart Note the nearly closed activation surface at 30 ms into the QRS complex. (Modified from "The Biophysical Basis for Electrocardiography," by R. Plonsey, in *CRC Critical Reviews in Bioengineering*, 1, 1, p.5, 1971, © The Chemical Rubber Co., 1971. Used by permission of The Chemical Rubber Co. Based on data by D. Durrer *et al.*, "Total excitation of the Isolated Human Heart," 1970, *Circulation*, 41, 899-912, by permission of the American Heart Association, Inc.)

© From J. G. Webster (ed.), *Medical instrumentation: application and design*. 3rd ed. New York: John Wiley & Sons, 1998.

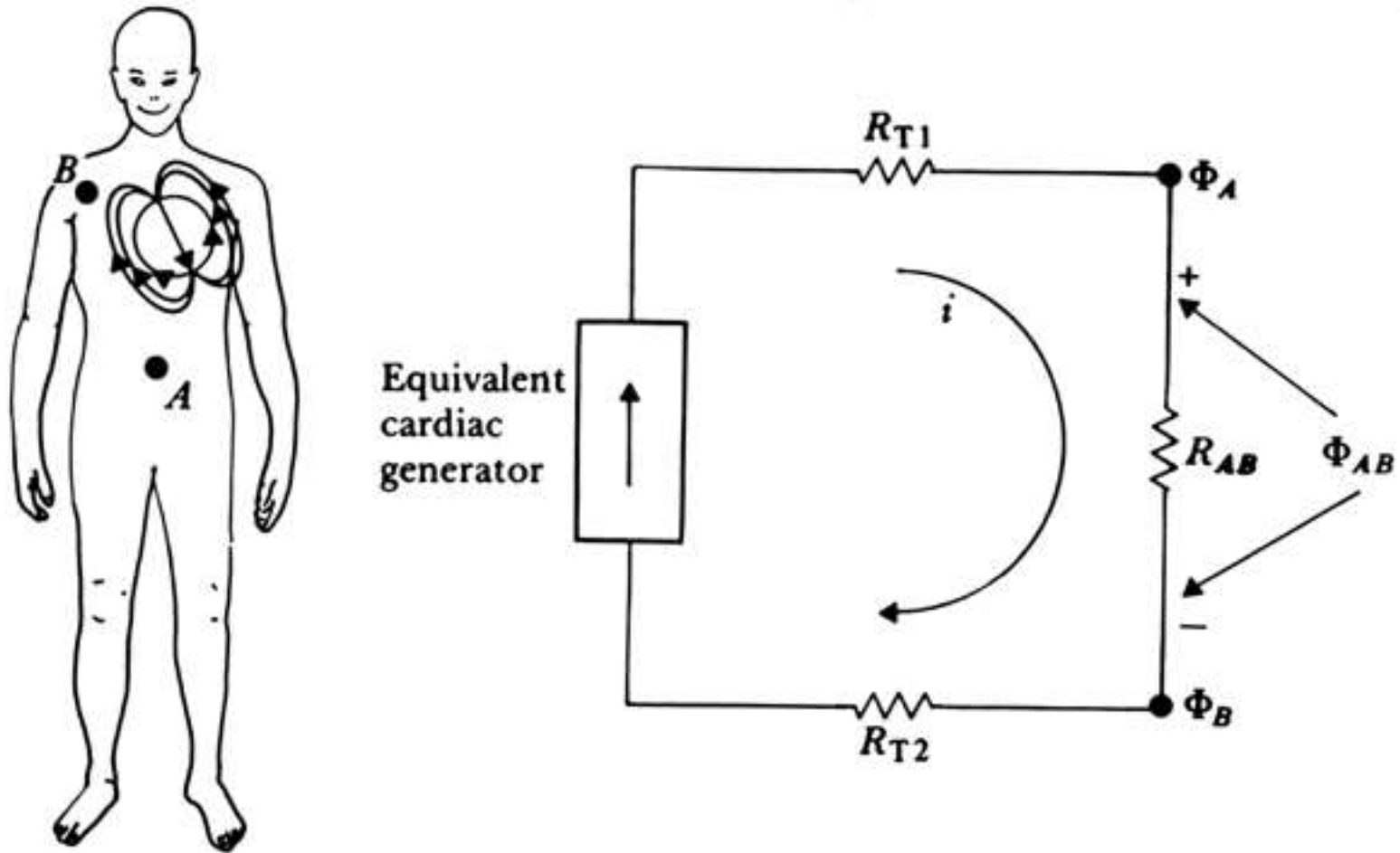
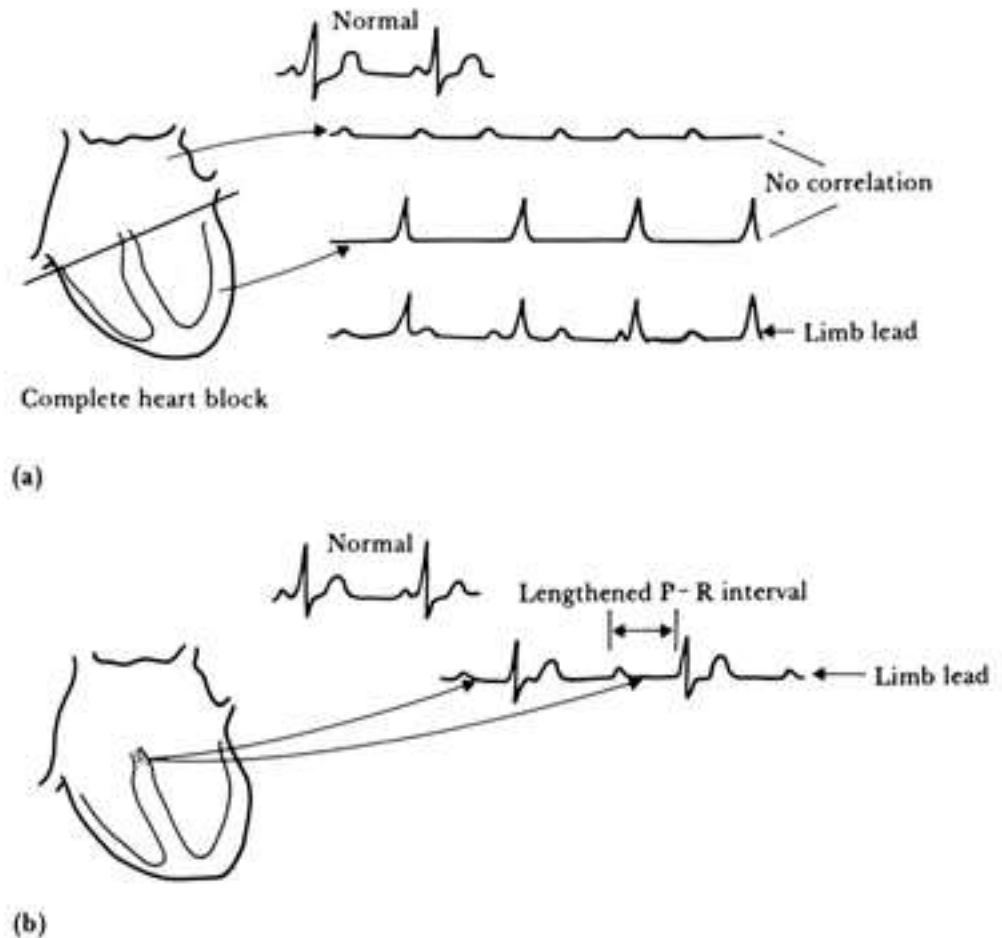


Figure 4.16 The electrocardiography problem Points A and B are arbitrary observation points on the torso, R_{AB} is the resistance between them, and R_{T1} , R_{T2} are lumped thoracic medium resistances. The bipolar ECG scalar lead voltage is $\phi_A - \phi_B$, where these voltages are both measured with respect to an indifferent reference potential.

Figure 4.17 Atrioventricular block

(a) Complete heart block. Cells in the AV node are dead and activity cannot pass from atria to ventricles. Atria and ventricles beat independently, ventricles being driven by an ectopic (other-than-normal) pacemaker. (B) AV block wherein the node is diseased (examples include rheumatic heart disease and viral infections of the heart). Although each wave from the atria reaches the ventricles, the AV nodal delay is greatly increased. This is first-degree *heart block*. (Adapted from Brendan Phibbs, *The Human Heart*, 3rd ed., St. Louis: The C. V. Mosby Company, 1975.)



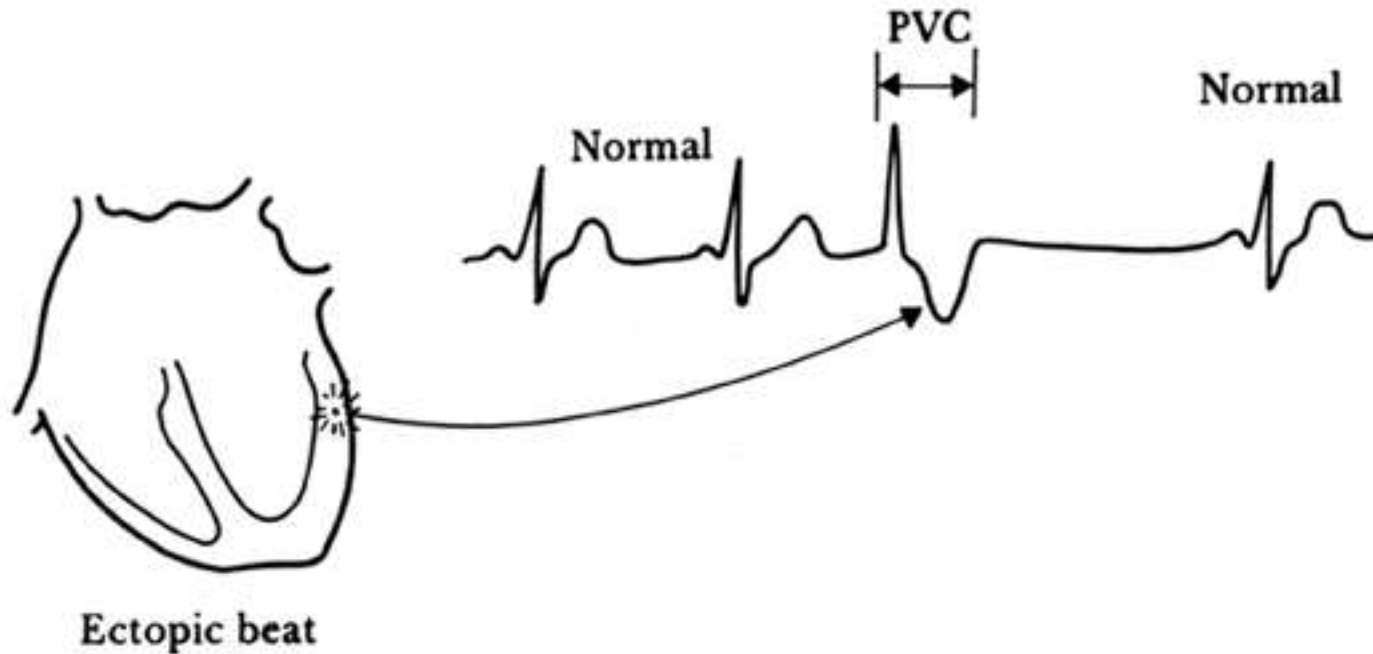


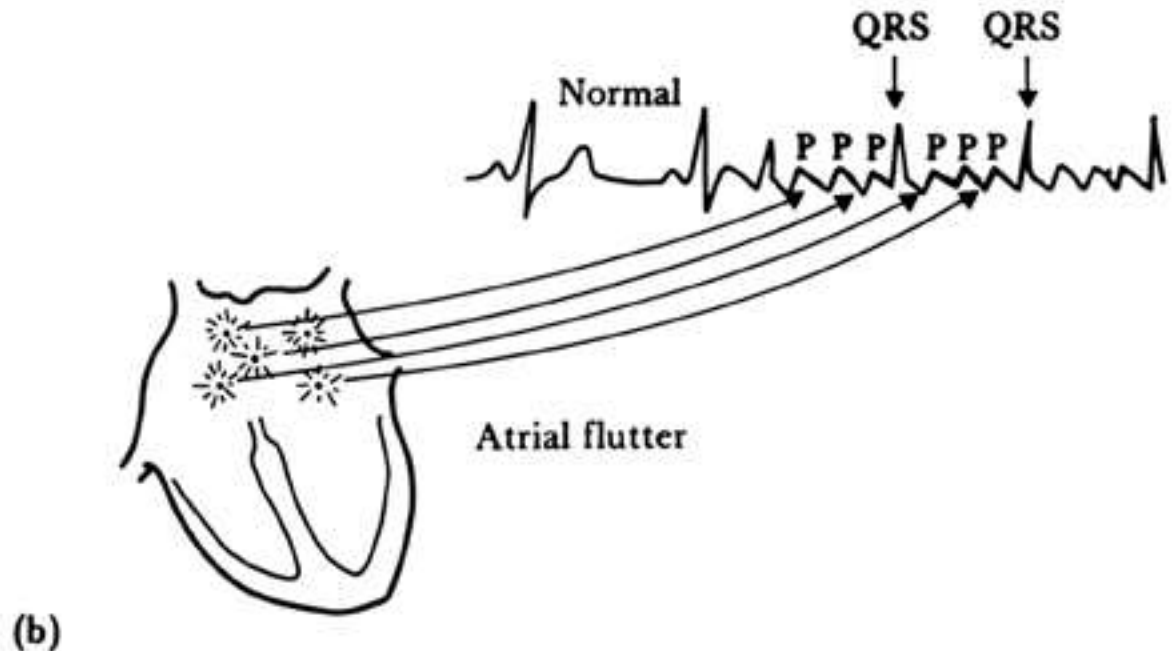
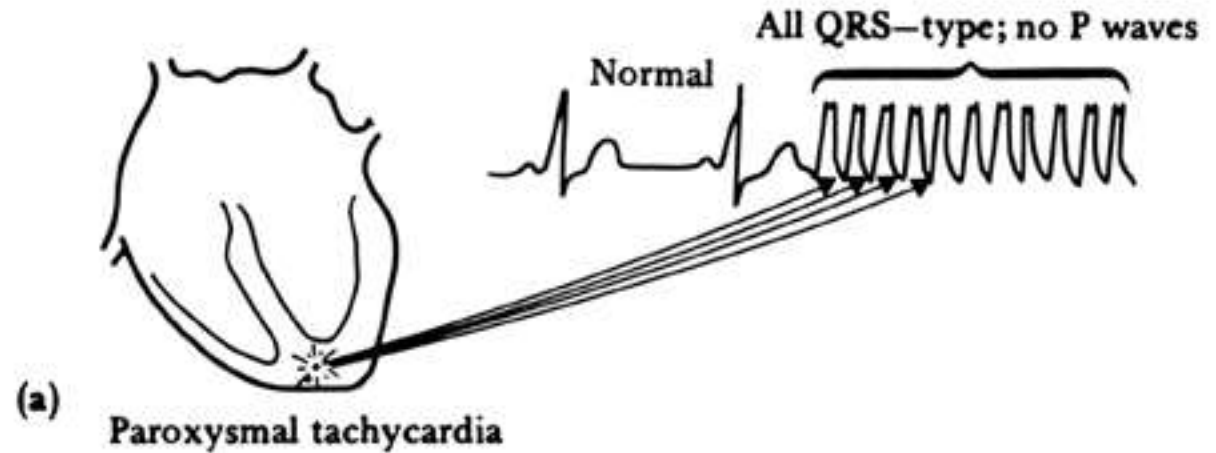
Figure 4.18 Normal ECG followed by an ectopic beat An irritable focus, or *ectopic pacemaker*, within the ventricle or specialized conduction system may discharge, producing an extra beat, or *extrasystole*, that interrupts the normal rhythm. This extrasystole is also referred to as a premature ventricular contraction (PVC). (Adapted from Brendan Phibbs, *The Human Heart*, 3rd ed., St. Louis: The C. V. Mosby Company, 1975.)

Figure 4.19 (a)

Paroxysmal tachycardia.

An ectopic focus may repetitively discharge at a rapid regular rate for minutes, hours, or even days. (B) Atrial flutter.

The atria begin a very rapid, perfectly regular "flapping" movement, beating at rates of 200 to 300 beats/min. (Adapted from Brendan Phibbs, *The Human Heart*, 3rd ed., St. Louis: The C. V. Mosby Company, 1975.)



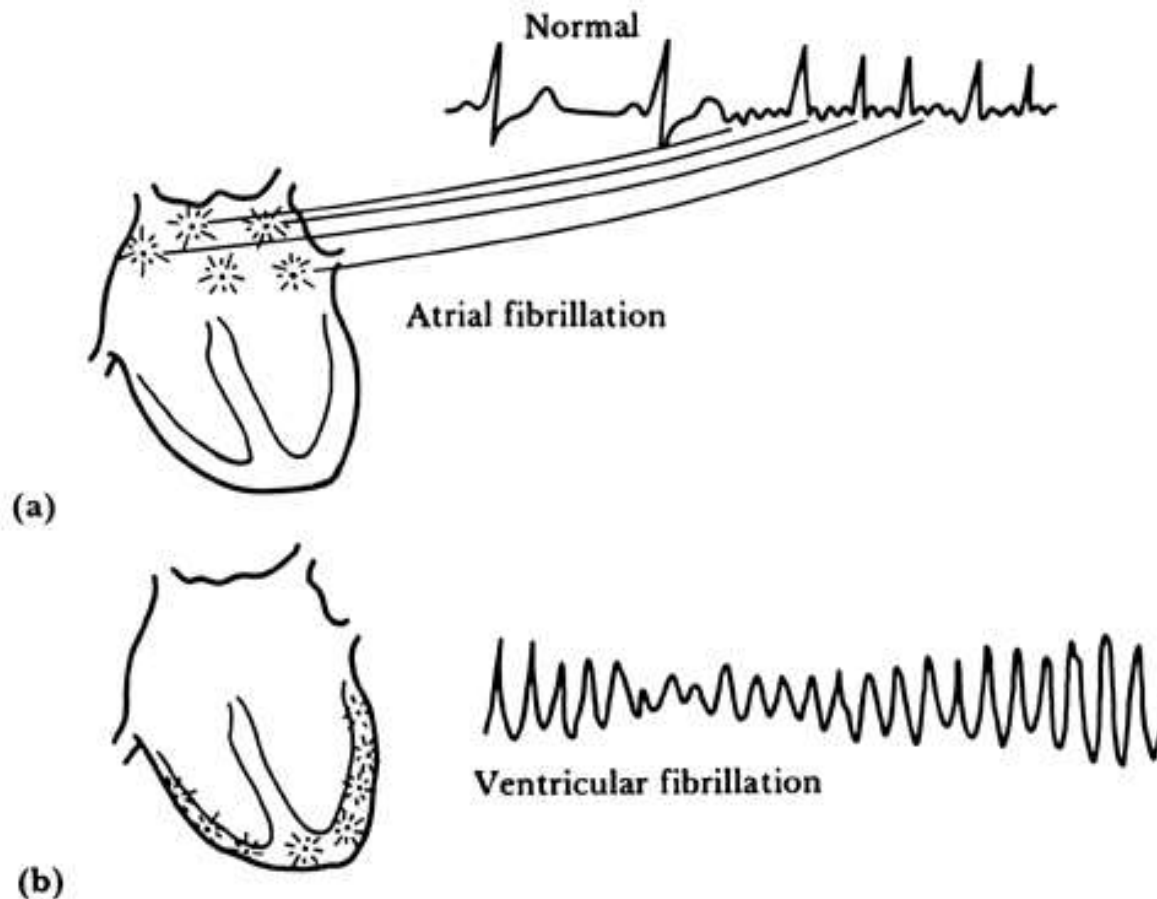


Figure 4.20 (a) Atrial fibrillation. The atria stop their regular beat and begin a feeble, uncoordinated twitching. Concomitantly, low-amplitude, irregular waves appear in the ECG, as shown. This type of recording can be clearly distinguished from the very regular ECG waveform containing atrial flutter. (b) Ventricular fibrillation. Mechanically the ventricles twitch in a feeble, uncoordinated fashion with no blood being pumped from the heart. The ECG is likewise very uncoordinated, as shown (Adapted from Brendan Phibbs, *The Human Heart*, 3rd ed., St. Louis: The C. V. Mosby Company, 1975.)

© From J. G. Webster (ed.), *Medical instrumentation: application and design*. 3rd ed. New York: John Wiley & Sons, 1998.

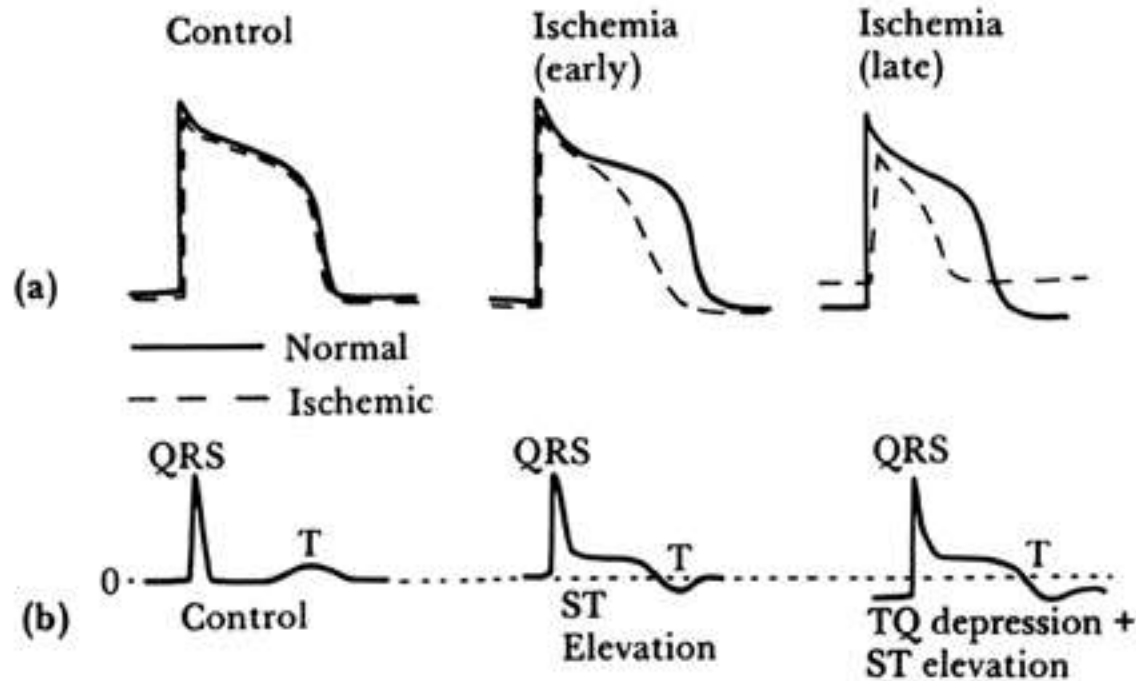


Figure 4.21 (a) Action potentials recorded from normal (solid lines) and ischemic (dashed lines) myocardium in a dog. Control is before coronary occlusion. (b) During the control period prior to coronary occlusion, there is no ECG S-T segment shift; after ischemia, there is such a shift. (From Andrew G. Wallace, "Electrophysiology of the Myocardium," in *Clinical Cardiopulmonary Physiology*, 3rd ed. New York: Grune & Stratton, 1969; used with permission of Grune & Stratton. Based on data by W. E. Sampson and H. M. Scher, "Mechanism of S-T Segment Alteration During Acute Myocardial Injury," 1960, *Circulation Research*, 8, by permission of The American Heart Association.)

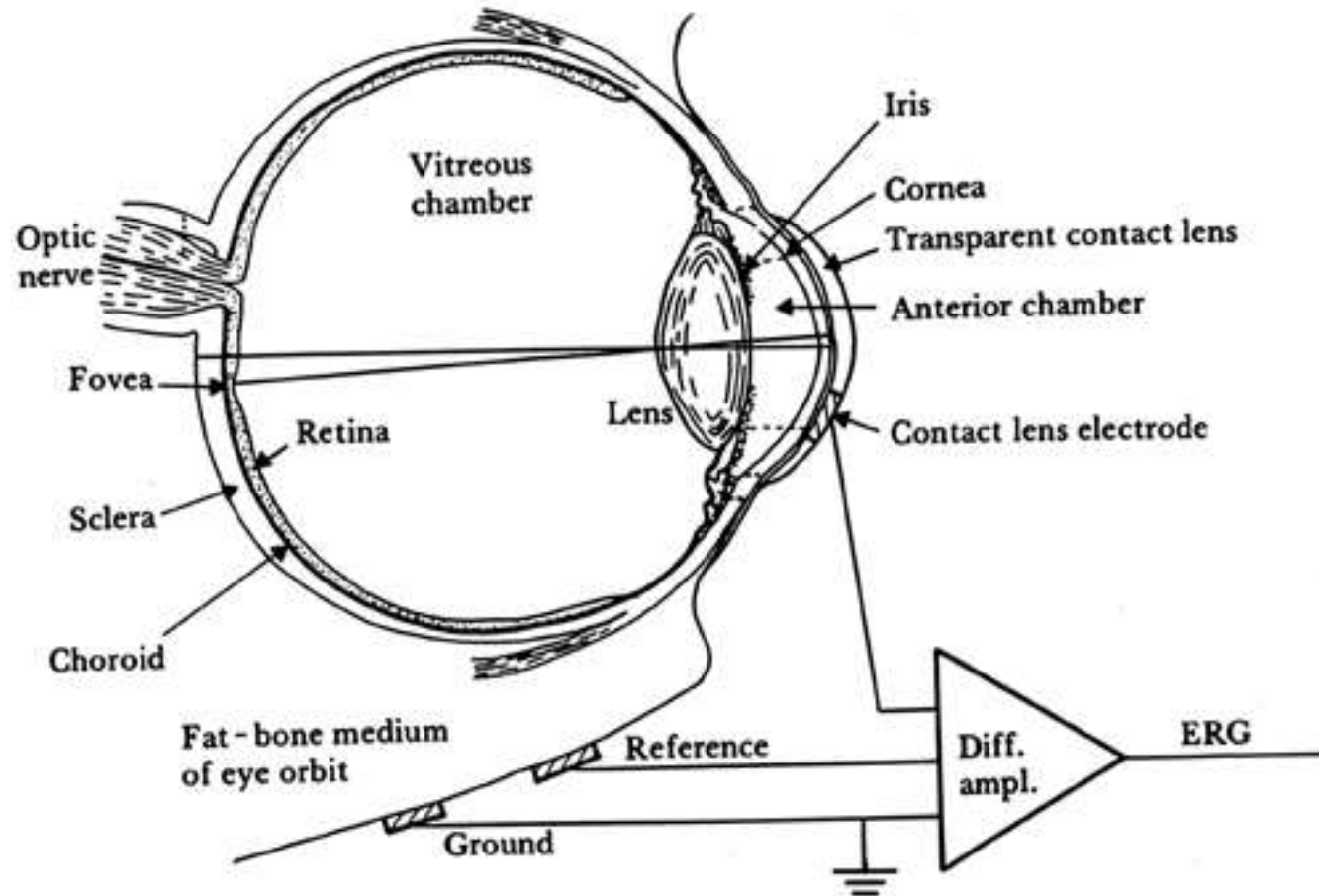


Figure 4.22 The transparent contact lens contains one electrode, shown here on horizontal section of the right eye. Reference electrode is placed on the right temple.

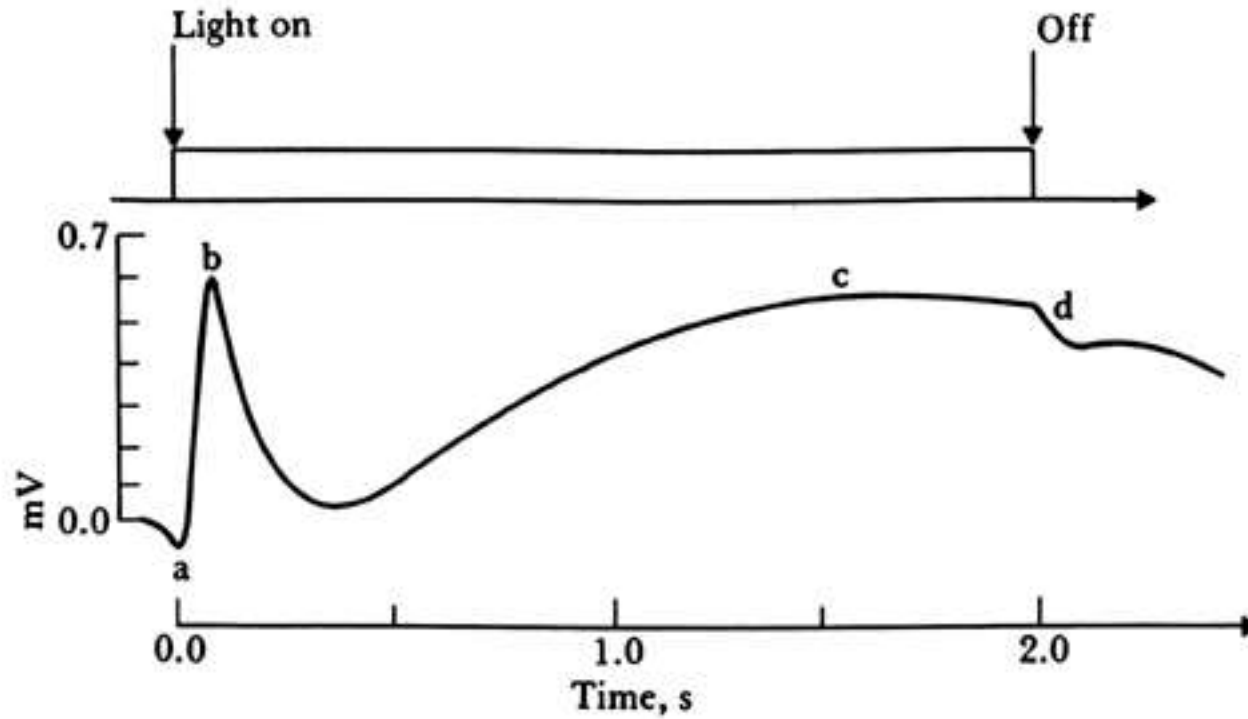
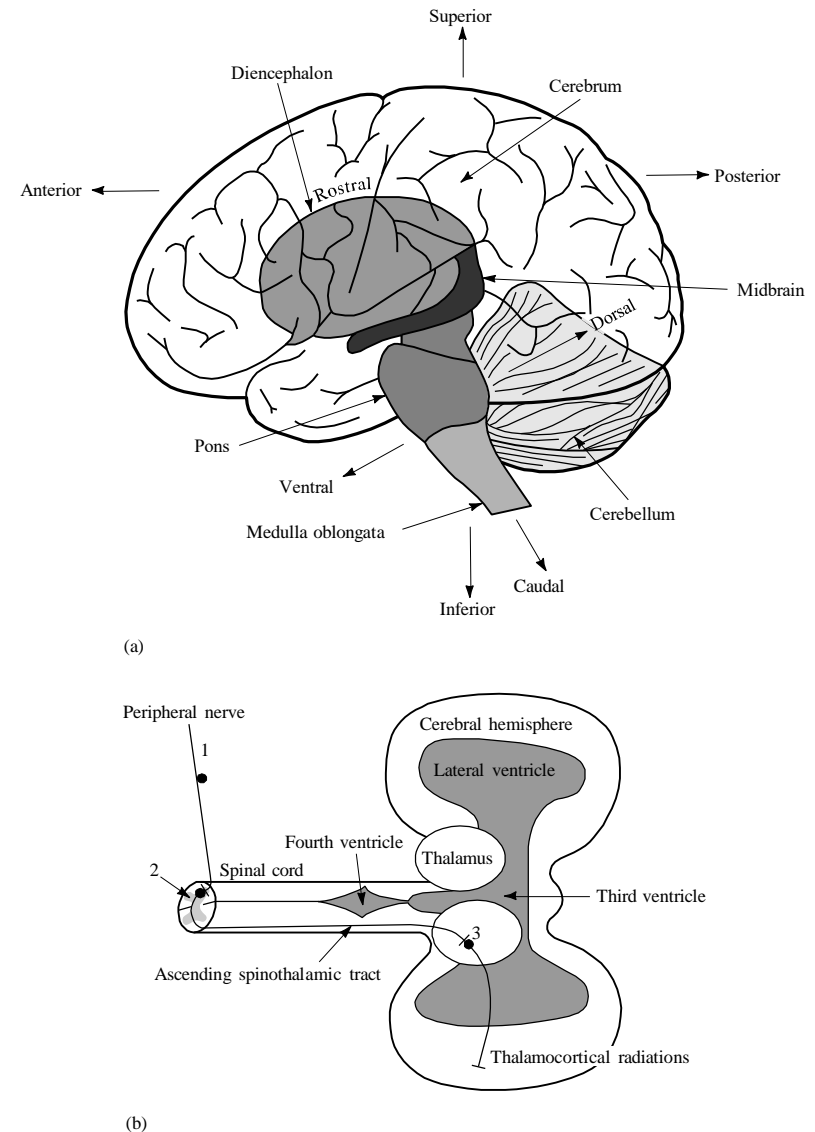


Figure 4.23 Vertebrate electroretinogram

Figure 4.24 (a) Anatomical relationship of brainstem structures (medulla oblongata, pons, midbrain, and diencephalons) to the cerebrum and cerebellum. General anatomic directions of orientation in the nervous system are superimposed on the diagram. Here the terms rostral (toward head), caudal (toward tail), dorsal (back), and ventral (front) are associated with the brainstem; remaining terms are associated with the cerebrum. The terms medial and lateral imply nearness and remoteness respectively, to or from the central midline axis of the brain. (b) A simplified diagram of the CNS showing a typical general sense pathway from the periphery (neuron 1) to the brain (neuron 3). Note that the axon of the secondary neuron (2) in the pathway decussates (crosses) to the opposite side of the cord. [Part (A) modified from Harry E. Thomas, *Handbook of Biomedical Instrumentation and Measurement*, 1974, p.254. Reprinted with permission of Reston Publishing Company, Inc. a Prentice-Hall company, 11480 Sunset Hills Road, VA 22090.]



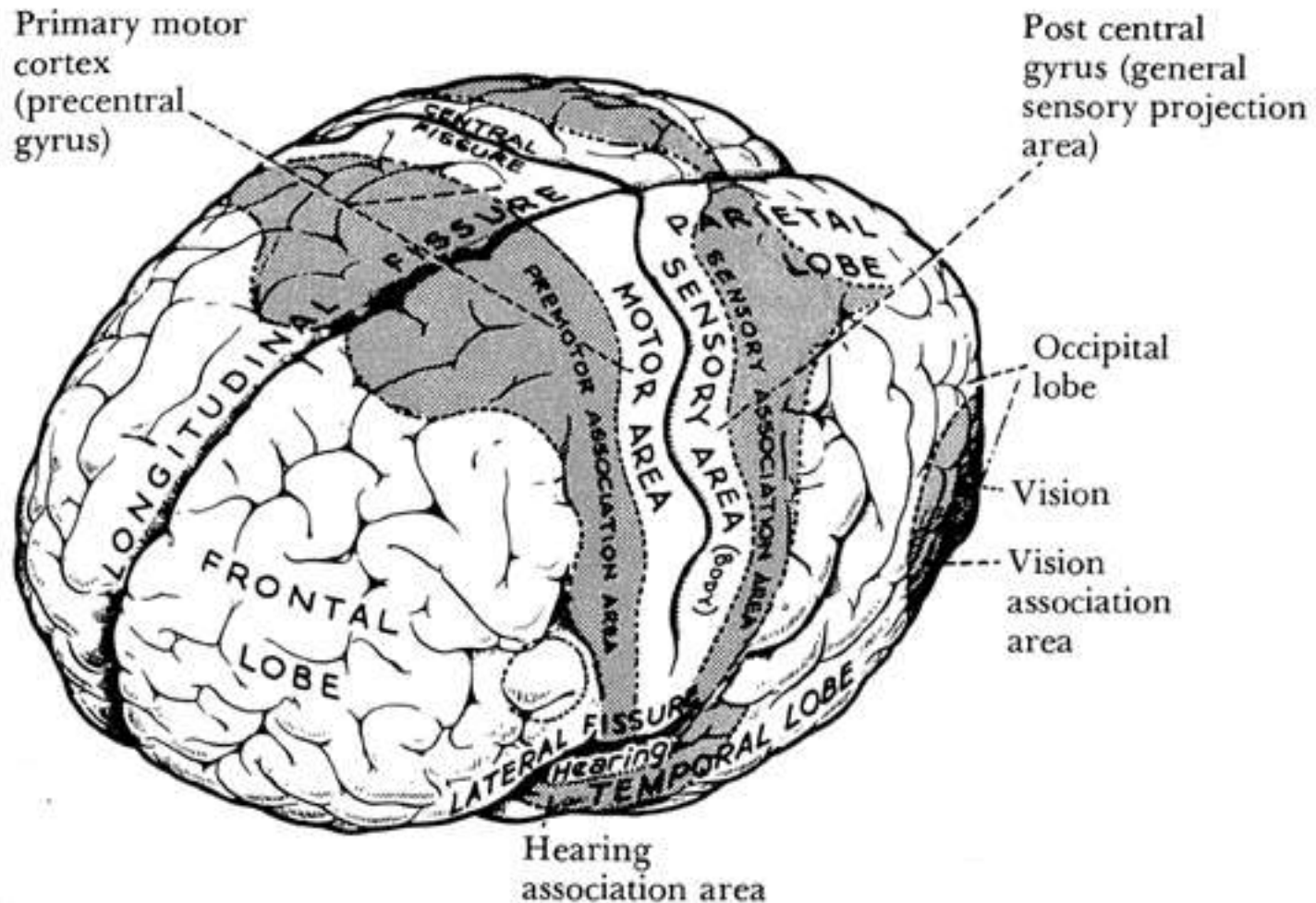


Figure 4.25 The cerebrum, showing the four lobes (frontal, parietal, temporal, and occipital), the lateral and longitudinal fissures, and the central sulcus. (From A. B. McNaught and R. Callander, *Illustrated Physiology*, 3rd ed., 1975. Edinburgh: Churchill Livingstone. Used with permission of Churchill Livingstone.)

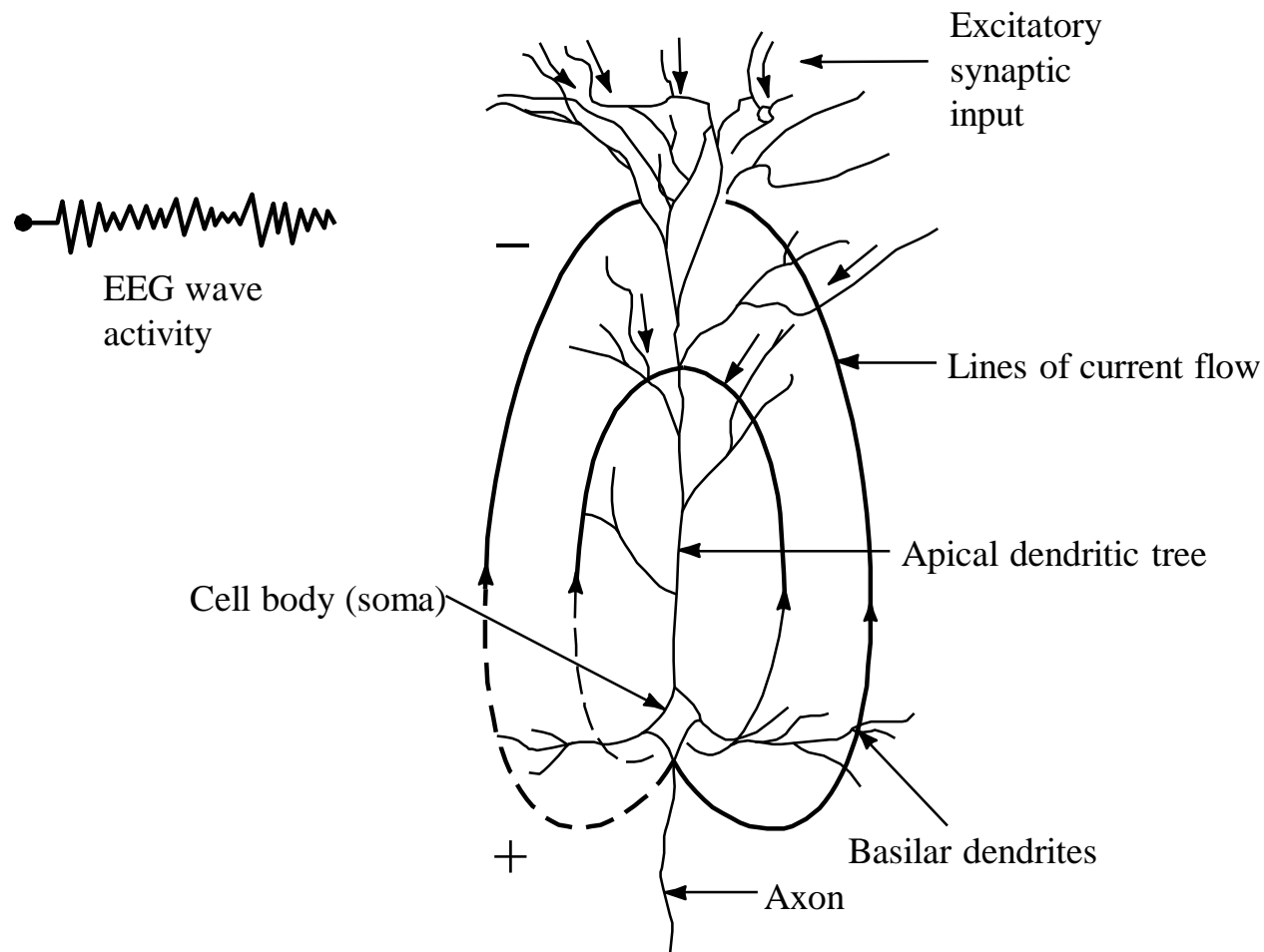


Figure 4.26 Electrogenesis of cortical field potentials for a net excitatory input to the apical dendritic tree of a typical pyramidal cell. For the case of a net inhibitory input, polarity is reversed and the apical region becomes a source (+). Current flow to and from active fluctuating synaptic knobs on the dendrites produces wave-like activity. See text.

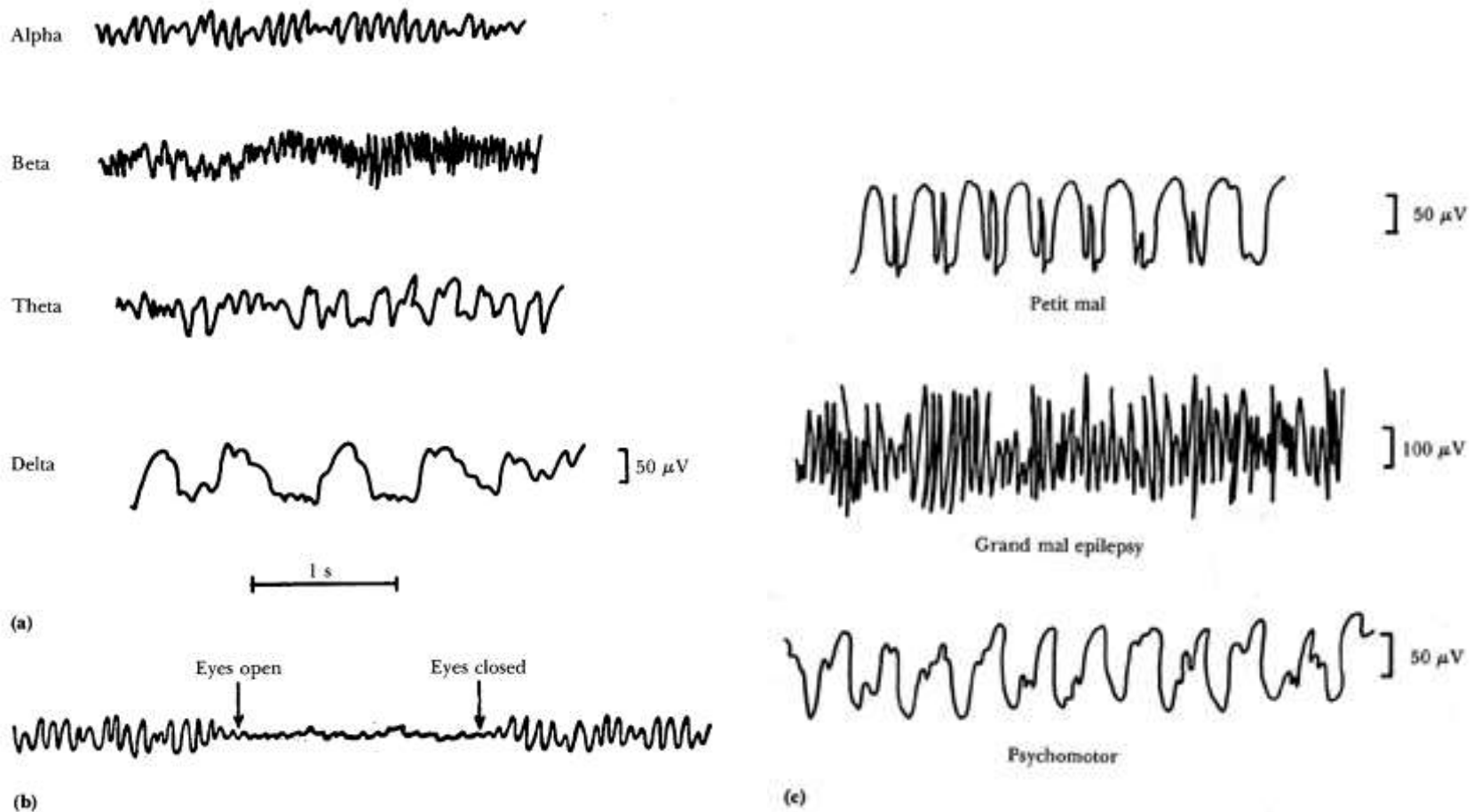


Figure 4.27 (a) Different types of normal EEG waves. (b) Replacement of alpha rhythm by an asynchronous discharge when patient opens eyes. (c) Representative abnormal EEG waveforms in different types of epilepsy. (From A. C. Guyton, *Structure and Function of the Nervous System*, 2nd ed., Philadelphia: W.B. Saunders, 1972; used with permission.)

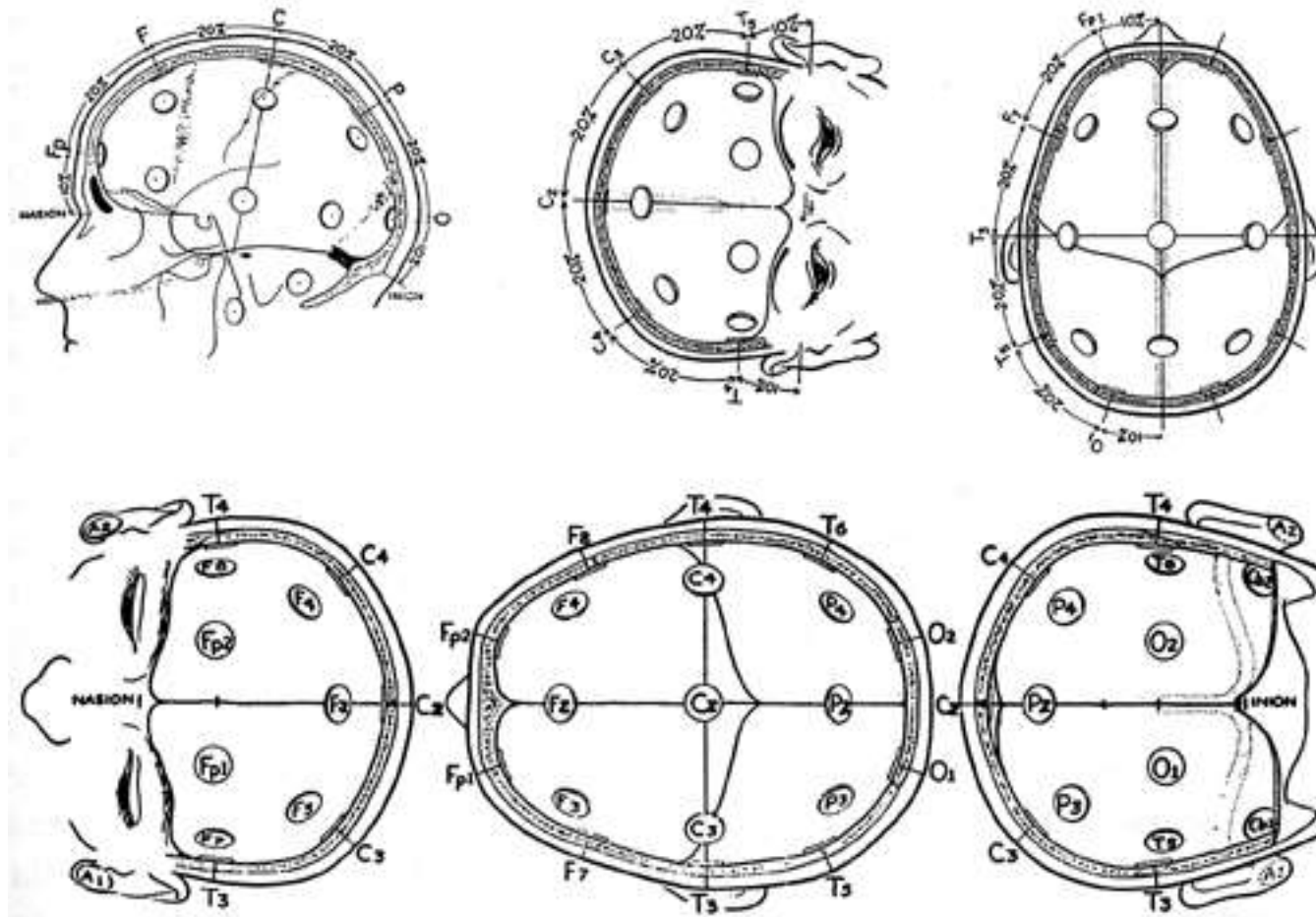


Figure 4.28 The 10-20 electrode system This system is recommended by the International Federation of EEG Societies. (From H. H. Jasper, "The Ten-Twenty Electrode System of the International Federation in Electroencephalography and Clinical Neurophysiology," *EEG Journal*, 1958, 10 (Appendix), 371-375.)

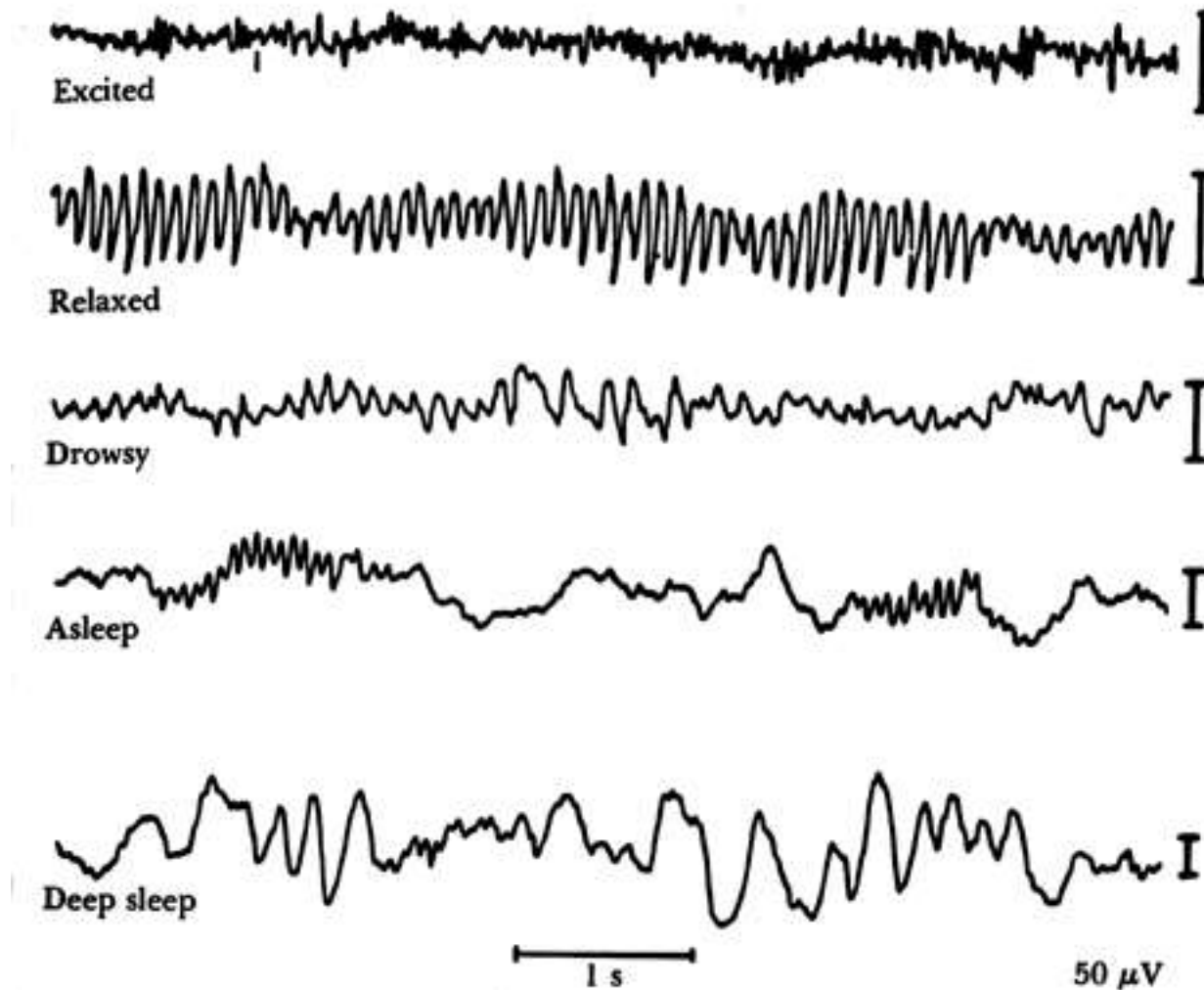


Figure 4.29 The electroencephalographic changes that occur as a human subject goes to sleep The calibration marks on the right represent 50 μV . (From H. H. Jasper, "Electroencephalography," in *Epilepsy and Cerebral Localization*, edited by W. G. Penfield and T. C. Erickson. Springfield, IL: Charles C. Thomas, 1941.)